Pulmonology 2021;27(1):14–25

PULMONOLOGY

www.journalpulmonology.org

ORIGINAL ARTICLE

Low dose computed tomography of the lung for detection and grading of interstitial lung disease: A systematic simulation study

S. Ley[c,f,h,*], L. Fidler[b], H. Schenk[c], M. Durand[d,f], T. Marras[e], N. Paul[f], S. Shapera[g], S. Mittoo[a]

[a] *Department of Rheumatology, Mount Sinai Hospital, Toronto, Ontario, Canada*
[b] *Department of Medicine, University of Toronto, Toronto, Ontario, Canada*
[c] *Surgical Clinic Munich South, Munich, Bavaria, Germany*
[d] *Department of Radiology, Grey's Hospital, Pietermaritzburg, KwaZulu-Natal, South Africa*
[e] *Department of Respirology, Toronto Western Hospital, Toronto, Ontario, Canada*
[f] *Joint Department of Medical Imaging, Toronto General Hospital, Toronto, Ontario, Canada*
[g] *Department of Respirology, Toronto General Hospital, Toronto, Ontario, Canada*
[h] *Institute of Clinical Radiology, Ludwig Maximilians University, Munich, Germany*

Received 5 May 2020; accepted 2 June 2020
Available online 24 June 2020

KEYWORDS
Interstitial Lung Disease;
Computed Tomography;
Low-dose;
Simulation study;
Diagnostic performance

Abstract
Purpose: HRCT is the preferred imaging technique to evaluate Interstitial-Lung-Disease. Optimal Low-Dose-Computed-Tomography protocol for monitoring ILD with lowest radiation dose and optimal diagnostic accuracy and image quality unknown.
Methods: 28 Patients underwent HRCT. Image reconstructions with varying combinations of tube current (50mA, 20mA, 15 mA, 10mA) and image-thickness/increment (1/1mm, 2/2mm, 3/2.4mm, 5/4mm) were simulated from raw data. 448 CTs evaluated by 2 readers on image quality and ILD-specific features (ground glass opacification (ggo), honeycombing (hc), reticulation (ret)).
Results: Reduced dose settings with 20 mA did not show any significant difference to standard dose settings for all parameters in reader 1, while results were significantly altered in reader 2. Slice thickness did not significantly influence rating of typical ILD features like ggo, hc, ret or total disease extent. The correct differentiation between UIP and NSIP could be made on all dose settings and with all slice thickness. It was even found, that an increased slice thickness can compensate for the noise associated image quality degradation. Overall, for ggo detection a combination of 20 mA and 3 or 5 mm slice thickness was not different to the original evaluation.

* Corresponding author.
E-mail address: ley@gmx.net (S. Ley).

https://doi.org/10.1016/j.pulmoe.2020.06.004

Conclusions: Assessment of ILD specific CT features down to 20 mA and a slice thickness of 3 or 5 mm is feasible.

Introduction

Interstitial lung disease (ILD) encompasses a heterogeneous group of disorders affecting the lung parenchyma that can lead to poor quality of life, hospitalization, and death.[1–3] Pulmonary function tests (PFTs) and chest X-rays (CXRs) have insufficient sensitivity to identify early ILD. Thoracic high-resolution computed tomography (HRCT) is the preferred method to detect and differentiate between the different forms of interstitial lung disease, being classified as usual interstitial pneumonia (UIP), probable UIP, indeterminate for UIP and alternative diagnosis (like non-specific interstitial pneumonia (NSIP)).[4–6] In lieu of a surgical biopsy, HRCT is an accepted gold standard for the diagnosis of ILD when certain specific findings are present.[5–8] Both UIP and NSIP can exhibit reticulation and traction bronchiectasis on chest HRCT; distinguishing radiologic features between these two subsets includes a greater degree of ground glass opacities (GGO) relative to reticulation in NSIP compared to UIP and the presence of honeycombing (HC) in UIP.[5,6]

HRCT is defined as a slice thickness less than 1.5 mm using a high-frequency reconstruction kernel.[9] To achieve diagnostic images a certain amount of radiation dose has to be applied to outweigh the image noise. So far, no official recommendations exist regarding latest noise reduction techniques like iterative reconstruction. This may be due to the fact, that each CT vendor uses different algorithms and the inter-study results show varying results of diagnostic accuracy based on the strength of image post-processing.

In light of the malignancy risk associated with exposure to cumulative doses of ionized radiation exposure, there is a trend for clinicians to request lower radiation dose protocols to monitor for ILD progression. These protocols tend to involve helical acquisition of CT data using reduced X-ray exposure parameters.[10] This is particularly relevant in patients with ILD who are already at an increased risk of developing pulmonary malignancy.[11] Especially repeated, long-term CT chest imaging in adults over 20–30 year periods, has been associated with non-trivial doses of radiation, exceeding that of nuclear plant workers and atomic bomb survivors.[12] For imaging of the lung parenchyma – as a high contrast tissue – a high kVp is recommended. Therefore, reduction of radiation dose with CT imaging is achieved by either reducing tube current and/or increasing the image slice interval (i.e. leaving gaps between slices). However, changes in tube current and image slice interval compromise image quality, negatively impact disease detection and estimated disease extent.[13,14] Research focused on finding the appropriate balance between CT imaging radiation exposure and optimal image quality is desperately needed. The problem with the design of systematic dose reduction studies is that a repeated CT examination of the same subject is unethical (and would also mean different breath-holds compromising image comparability). Past studies evaluating LDCT imaging in ILD have therefore chosen imaging parameters arbitrarily, failing to establish an optimal LDCT protocol for detecting and distinguishing ILD and its subsets (UIP and NSIP).

As there is no study out evaluating a steady decrease in dose in the same patient, the aim of this study was to find an optimal imaging protocol to identify and grade specific features of ILD in comparison to standard 3d-HRCT.

Materials and methods

Patient and sample population

Patients treated at the Toronto General Hospital-ILD clinic, a tertiary academic referral clinic, were approached for study enrolment between July 2012 and April 2013. Oral and written consent was recorded when the patients were approached while visiting the clinic for regularly scheduled appointments. Patient consent records were stored securely with their study records. Adult patients ($\geq$18 years of age) with a diagnosis of IPF, idiopathic NSIP, or connective tissue disease (CTD)-ILD and who required a thoracic CT at their visit were included. Patients with a history of pneumotoxic medication use, environmental exposures, granulomatous lung disease (i.e. sarcoidosis) or other idiopathic interstitial pneumonias were excluded from this study. A diagnosis of IPF was based on criteria outlined by American Thoracic Society guidelines.[5,6] A rheumatologist evaluated all patients to confirm the presence of a CTD (rheumatoid arthritis, systemic sclerosis, idiopathic inflammatory myositis, Sjogren's syndrome, mixed connective tissue disease, systemic lupus erythematosus, or undifferentiated connective tissue disease).

Ethics approval was obtained prior to patient enrolment from both the BLINDED FOR REVIEW Research Ethics Board and the BLINDED FOR REVIEW Research Ethics Board.

CT image acquisition and assessment

Patients were scanned in the prone position during full inspiration. Average patient anterior–posterior (AP) and left–right (LR) body size was 253.8 mm (*S.E.* = 8.3) and 328.3 mm (*S.E.* = 6.7) respectively. Images were acquired with a 64 mm $\times$ 0.5 mm detector configuration using two CT scanners: Aquilion 64 (n = 26) or Aquilion One (n = 5) (both Toshiba Medical Systems, Ottawara, Japan). Image acquisition was done with the clinical routine protocol (120 kVp,

Table 1 Summary of CT acquisitions and simulation parameters.

Nr patients	Original dose	Simulated dose	Slice thickness/increment	Nr datasets
8	Automatic dose (115–212 mA)	SD 30 SD 40 SD 50	1/1 mm 2/2 mm 3/2.4 mm 5/4 mm	128
20	50 mA	20 mA 15 mA 10 mA	1/1 mm 2/2 mm 3/2.4 mm 5/4 mm	320

0.5 s rotation time). The raw data from each clinical scan was stored and used for low dose simulation using the Toshiba low dose simulation software.[15] No iterative reconstruction techniques were used. Some original data were acquired using automatic dose exposure ($n = 8$, 115–212 mA – depending on body habitus), and others with fixed mA settings (50 mA). For low dose simulation, the noise levels were reconstructed for the following standard deviation (SD) of noise of 30, 40 and 50 Hounsfield Units (HU) (as allowed by the software). The fixed mA datasets were simulated at 20 mA, 15 mA and 10 mA. Reconstruction was done with various slice thicknesses/increments: 1 mm/1 mm, 2 mm/2 mm, 3 mm/2.4 mm, and 5 mm/4 mm (for the thicker slice thicknesses an overlap of 20% was chosen to allow for increased characterization benefit[16]). The reconstruction kernel was FC03 (soft tissue kernel) to reduce noise without limiting imaging characteristics known from CAD. This setting allowed for intra-individual comparison of the impact of dose reduction. As the same raw data set was used, there were no variations in physiological conditions, such as inspiratory depth and fluid content. Only one CT scan was performed on each study participant, thus no additional radiation burden was applied.

Overall, 28 patients with 4 different dose settings and 4 slice thickness/increment settings were reconstructed, in total 448 CT datasets were used for evaluation (Table 1).

The clinical dose CT dataset (original dose, no noise) with 1 mm slice thickness was used as reference standard.

All CT images were interpreted in random order and separately by a radiologist (reader 1) with over 15 years of experience in thoracic radiology, and one second year radiology resident (reader 2). Both were blinded to the patients' clinical history. Lung parenchyma was evaluated by individual lobe (right upper, right middle, right lower, left upper, lingua and left lower) for the presence of GGO, reticulation, and HC. Each lobe was scored for extent of these changes from 0 to 100% in 5% intervals. GGO was defined according to the Fleischner Glossary of Terms for Thoracic Imaging as an increase in lung attenuation without obscuring pulmonary vessels, reticulation as fine or thick reticular grid and thickened interlobular septa and honeycombing as peripheral cysts within a coarse reticulation.[17]

An overall estimate of image quality, number of lobes involved and total percent of diseased lung was provided by the readers for each patient's series. Image quality was rated on a scale from 1 to 4, with 1 indicating excellent image quality without any artefacts; 2 indicating good image quality with minor streak artefacts without limiting image interpretation; 3 indicating moderate image quality with more severe streak artefacts limiting image interpretation; and 4 indicating bad image quality with severe artefacts significantly impairing image interpretation. The radiologic pattern was recorded as UIP, NSIP, or non-classifiable fibrosis for all CT scans at each LDCT series. UIP and NSIP were defined in accordance with ATS guidelines for IPF and the idiopathic interstitial pneumonias (IIPs) respectively.[5,6] As mentioned above, HRCT scans with the highest tube current (clinical established dose levels), 1 mm slice thickness were established as the conventional (reference) standard.

The optimal LDCT was selected based on the following three features:(1) diagnostic accuracy, (2) image quality and (3) delivered radiation dose between series. Diagnostic accuracy was considered the most important operating characteristic, given that the overall radiographic pattern often influences clinical diagnosis and treatment decisions. Image quality influences the perception of other CT imaging features (i.e. GGO, reticulation and disease) and hence was chosen as the second most important factor. LDCT imaging series' with similar diagnostic accuracy and image quality were differentiated based on delivered radiation dose, with the lowest dose series deemed most optimal.

Statistical analysis

For statistical analysis the average scores for total involvement of GGO, reticulation and HC across all lobes were enumerated. Also, the total disease extent was used (average of the sum of all three types of radiographic changes between the left and right lungs). Mixed linear models were used to investigate the effects of different series on operating characteristics and imaging features. The estimation method ''REML'' (residual (restricted) maximum likelihood) was used.

Statistical evaluation was done on a per-patient basis using SAS Version 9.3, Cary, North Carolina, USA. A local level of significance (p) of <0.05 was considered statistically significantly.

Results

Patient population and baseline HRCT imaging

Of 35 patients approached for study involvement, seven were excluded (4 due to difficulty attaining stored CT images, 2 with hypersensitivity pneumonitis, and 1 with

Table 2 Demographic, disease, and pulmonary characteristics of 28 patients with ILD.

Demographics	
Females, %	56
Age [years], mean (S.E.)	60.3 (2.8)
Ever smoked tobacco, %	36.0
Body size anterior–posterior [mm], mean (S.E.)	253.8 (8.3)
Body size lateral–radial [mm], mean (S.E.)	328.3 (6.7)
Disease diagnosis	
Idiopathic pulmonary fibrosis, %	20
Non IPF, %	80
Pulmonary function test	
Forced vital capacity, % predicted, mean (S.E.)	66.3 (4.1)
Total lung capacity, % predicted, mean (S.E.)	69.8 (3.2)
Diffusing capacity of carbon monoxide, % predicted, mean (S.E.)	67.3 (3.1)

sarcoidosis). Among 28 patients evaluated (56% female) with approximately one-third having a past history of cigarette smoking (Table 2). A clinical diagnosis of IPF and NSIP were made in 20%, and 80% patients respectively. Routine clinical HRCT imaging (120 kV, fixed 50 mA or dose modulation 115–212 mA, 1 mm slice thickness) (Table 1), was reported as UIP in 6 cases (24%) and NSIP in 19 (76%) cases. In total, 448 individual CT scans were generated, reviewed and analyzed.

To provide the utmost insight into the data, the evaluation results of reader 1 are provided in Table 3. Given the huge amount of primary data, ''Results'' section is focused on the statistical results. As mentioned above, for each radiological feature the percentage of affected/diseased lung was visually assessed for each dose level and slice thickness.

Ground glass opacities (GGO)

The overall analysis found a significant ($p < 0.001$) influence of dose on the correct findings for GGOs (Fig. 1). In detail, for reader 1, the second dose level was not significantly different from the reference standard ($p = 0.21$), while dose level three and four showed significant differences ($p = 0.0003$ and $p < 0.0005$, respectively) (Table 4). For reader 2, even the second dose level led to a significant difference in evaluation of the amount of ggo pattern.

The overall analysis found no significant ($p = 0.25$) influence of slice thickness on the correct findings for GGOs for reader 1. In detail, the 2 mm slice thickness resulted in a p-value of 1, 3 mm and 5 mm in $p = 0.89$ and $p = 0.19$, respectively. The combined evaluation of reader 1 and reader 2 confirmed the findings, that a slice thickness of 3 mm showed no significant difference ($p = 0.55$).

Honey combing (HC)

The overall analysis found a significant ($p = 0.002$ and $p < 0.0001$, respectively) influence of dose on the correct findings for HC. In detail, for reader 1 the second and third dose level were not significantly different ($p = 0.29$ and $p = 0.11$, respectively), while dose level four showed significant difference ($p = 0.002$). For the combined evaluation the second dose level was borderline not significantly different ($p = 0.55$).

The overall analysis for reader 1 found no significant ($p = 0.30$) influence of slice thickness on the correct findings for HC. In detail, the 2 mm slice thickness resulted in a p-value of 1, 3 mm and 5 mm in $p = 1$ and $p = 0.86$, respectively. For reader 2 and the combined analysis a slice thickness of 3 mm showed no significant difference on the evaluation of HC, $p = 0{,}64$ and $p = 0.68$, respectively.

Reticulation (RET)

The overall analysis found no significant ($p = 0.38$) influence of dose on the correct findings for reticulation (Fig. 2). In detail, for reader 1 the second dose level was not significantly different ($p = 0.86$), dose level three and four showed p-values of 0.85 and $p = 0.14$, respectively. For reader 2, all reduced dose levels showed a significant difference ($p < 0.0001$).

The overall analysis (reader 1) found no significant ($p = 0.59$) influence of slice thickness on the correct findings for reticulation. In detail, the 2 mm slice thickness resulted in a p-value of 1, 3 mm and 5 mm in $p = 0.98$ and $p = 0.94$, respectively. For reader 2 the slice thickness had no significant impact on detection rate (mean $p = 0.14$).

Total disease extend

The overall analysis found a significant ($p < 0.0001$ and $p = 0.02$, respectively) influence of dose on the correct findings for total disease extend. In detail, for reader 1 the second dose level was not significantly different ($p = 0.61$), dose level three and four showed p-values of <0.0001 and $p < 0.0001$, respectively.

The overall analysis found a significant ($p = 0.024$ and $p = 0.003$, respectively) influence of slice thickness on the correct total disease extend. In detail, for reader 1 the 2 mm slice thickness resulted in a p-value of 1, 3 mm and 5 mm in $p = 0.98$ and $p = 0.017$, respectively.

Image quality

The overall analysis found a significant ($p < 0.0001$) influence of dose on image quality. In detail, was the second dose level significantly different ($p < 0.0001$), dose level three and four showed p-values of <0.0001 and $p < 0.0001$, respectively.

The overall analysis found a significant ($p < 0.0001$) influence of slice thickness on image quality for both readers. In detail, for reader 1 the 2 mm slice thickness resulted in a p-value of =0.08, 3 mm and 5 mm in $p < 0.001$ and $p = 0.0002$, respectively.

Diagnosis

Using a logistic regression model the likelihood for establishing the correct diagnosis was calculated (Fig. 3).

Table 3 Individual results of reader 1 for the different dose levels (doses 1–4) and parameters: ground glass opacification (GGO), honeycombing (HC), reticulations (Ret) and total amount of disease (total).

Pat.	Dose 1				Dose 2				Dose 3				Dose 4			
	GGO	HC	Ret	Total	GGO	HC	Ret	Total	GGO	HC	Ret	Total	GGO	HC	Ret	Total
1 mm																
P1	16	0	16	20	16	0	16	20	21	0	18	23	19	0	18	23
P2	10	18	17	25	10	18	17	25	10	18	17	25	10	18	17	25
P3	37	0	23	60	37	0	23	60	37	0	23	60	37	0	23	60
P5	38	0	6	60	38	0	6	60	38	0	6	60	38	0	6	60
P6	5	0	14	15	8	0	14	20	3	0	14	15	5	0	14	15
P7	12	6	47	45	12	6	47	45	11	6	47	45	14	6	47	45
P8	7	15	22	25	7	15	22	20	7	15	22	20	14	15	22	28
P9	5	0	4	5	5	0	4	5	13	0	4	10	19	0	4	13
P10	8	3	16	10	3	3	16	10	67	3	13	70	100	2	12	100
P11	23	23	27	30	23	23	27	30	33	23	27	38	37	23	27	38
P13	52	0	7	55	100	0	7	100	100	0	8	100	100	0	50	100
P14	100	0	100	100	100	0	100	100	100	0	100	100	100	0	100	100
P15	39	0	5	43	39	0	5	43	58	0	5	58	100	0	13	100
P16	4	28	0	35	32	18	0	35	100	13	0	65	100	13	0	65
P17	58	33	10	55	58	33	10	55	65	33	10	60	73	33	10	65
P19	45	0	35	50	45	0	35	50	58	0	35	60	70	0	35	68
P20	31	0	7	30	31	0	7	30	31	0	7	30	35	0	7	33
P23	10	60	3	60	10	60	3	60	10	60	3	60	17	60	3	65
P24	30	0	0	35	30	0	0	35	30	0	0	35	35	0	0	38
P25	3	60	0	60	7	60	0	60	28	60	0	80	100	47	0	80
P26	21	0	23	33	36	0	29	43	100	0	29	75	100	0	31	75
P27	20	48	0	70	23	48	0	70	27	48	0	75	37	48	0	83
P28	18	0	13	10	18	0	13	10	18	0	13	10	18	0	13	10
P30	5	4	0	5	5	4	0	5	5	4	0	5	7	4	0	10
P31	65	0	53	75	65	0	53	75	60	0	53	73	78	0	53	85
P32	45	43	7	75	45	43	7	75	45	43	7	75	45	43	7	75
P33	40	0	37	65	73	0	37	80	87	0	37	90	100	0	37	100
P34	37	0	0	45	37	0	0	45	37	0	0	45	37	0	0	45
2 mm																
P1	16	0	16	20	16	0	16	20	16	0	16	20	19	0	18	23
P2	10	18	17	25	10	18	17	25	10	18	17	25	10	18	17	25
P3	37	0	23	60	37	0	23	60	37	0	23	60	37	0	23	60
P5	38	0	6	60	38	0	6	60	38	0	6	60	38	0	6	60
P6	5	0	14	15	3	0	14	15	5	0	14	15	5	0	14	15
P7	12	6	47	45	12	6	47	45	12	6	47	45	14	6	47	45
P8	7	15	22	25	7	15	22	20	7	15	22	20	11	15	22	23
P9	5	0	4	5	5	0	4	5	8	0	4	5	13	0	4	10
P10	8	3	16	10	4	3	16	10	33	3	16	35	100	2	13	100
P11	23	23	27	30	23	23	27	30	27	23	27	33	27	23	27	33
P13	52	0	7	55	48	0	7	50	48	0	7	50	100	0	7	100
P14	100	0	100	100	100	0	100	100	100	0	100	100	100	0	100	100
P15	39	0	5	43	39	0	5	43	48	0	5	45	97	0	10	95
P16	4	28	0	35	16	23	0	35	80	18	0	55	100	14	0	65
P17	58	33	10	55	58	33	10	55	58	33	10	55	62	33	10	58
P19	45	0	35	50	45	0	35	50	50	0	35	53	58	0	35	60
P20	31	0	7	30	31	0	7	30	31	0	7	30	31	0	7	30
P23	10	60	3	60	10	60	3	60	10	60	3	60	10	60	3	60
P24	30	0	0	35	30	0	0	35	30	0	0	35	30	0	0	35
P25	3	60	0	60	3	63	0	60	20	60	0	75	70	55	0	75
P26	21	0	23	33	26	0	25	35	50	0	25	50	60	0	31	65
P27	20	48	0	70	20	48	0	70	23	48	0	70	30	48	0	78
P28	18	0	13	10	18	0	13	10	18	0	13	10	18	0	13	10

Table 3 (*Continued*)

Pat.	Dose 1				Dose 2				Dose 3				Dose 4			
	GGO	HC	Ret	Total	GGO	HC	Ret	Total	GGO	HC	Ret	Total	GGO	HC	Ret	Total
P30	5	4	0	5	5	4	0	5	5	4	0	5	5	4	0	5
P31	65	0	53	75	65	0	53	75	65	0	53	75	68	0	53	75
P32	45	43	7	75	45	43	7	75	45	43	7	75	45	43	7	75
P33	40	0	37	65	40	0	37	65	47	0	37	70	88	0	37	90
P34	37	0	0	45	37	0	0	45	37	0	0	45	37	0	0	45
3 mm																
P1	16	0	16	20	21	0	16	28	19	0	18	23	19	0	19	23
P2	12	18	17	25	12	18	17	25	12	18	17	25	12	18	17	25
P3	37	0	23	60	37	0	123	60	37	0	23	60	37	0	23	60
P5	38	0	6	60	38	0	6	60	38	0	6	60	38	0	6	60
P6	5	0	14	15	3	0	14	15	5	0	14	15	5	0	14	15
P7	12	6	47	45	12	6	47	45	12	6	47	45	12	6	47	45
P8	7	15	22	20	7	15	22	20	7	15	22	20	7	15	22	20
P9	5	0	4	5	5	0	4	5	5	0	4	5	8	0	4	5
P10	8	3	16	10	8	3	16	10	8	3	16	10	70	3	16	70
P11	23	23	27	30	23	23	27	30	23	23	27	30	27	23	27	33
P13	52	0	7	55	52	0	7	55	48	0	7	50	63	0	7	70
P14	0	0	18	20	0	0	18	20	100	0	100	100	100	0	100	100
P15	39	0	5	43	39	0	5	43	39	0	5	43	82	0	8	75
P16	4	28	0	35	4	28	0	35	27	18	0	35	80	18	0	55
P17	58	33	10	55	58	33	10	55	58	33	10	55	58	33	10	55
P19	45	0	35	50	45	0	35	50	45	0	35	50	45	0	35	50
P20	31	0	7	30	31	0	7	30	31	0	7	30	31	0	7	30
P23	10	60	3	60	10	60	3	60	10	60	3	60	10	60	3	60
P24	30	0	0	35	30	0	0	35	30	0	0	35	30	0	0	35
P25	3	60	0	60	3	60	0	60	8	60	0	65	37	60	0	70
P26	21	0	23	33	21	0	23	33	36	0	23	43	50	0	31	60
P27	27	48	0	75	27	48	0	75	27	48	0	75	23	48	0	75
P28	18	0	13	10	18	0	13	10	18	0	13	10	18	0	13	10
P30	5	4	0	5	5	4	0	5	5	4	0	5	5	4	0	5
P31	65	0	53	75	65	0	53	75	65	0	53	75	65	0	53	75
P32	45	43	7	75	45	43	7	75	45	43	7	75	45	43	7	75
P33	40	0	37	65	40	0	37	65	40	0	37	65	50	0	37	70
P34	37	0	0	45	37	0	0	45	37	0	0	45	37	0	0	45
5 mm																
P1	19	0	18	28	26	0	18	35	19	0	18	23	19	0	19	23
P2	13	18	17	25	13	18	17	25	13	18	17	25	13	18	17	25
P3	37	0	23	60	38	0	25	60	38	0	25	60	38	0	25	60
P5	37	0	6	60	37	0	6	60	37	0	6	60	37	0	6	60
P6	5	0	14	15	7	0	14	20	5	0	14	15	5	0	14	15
P7	12	6	47	45	14	6	47	45	14	6	47	45	11	6	47	45
P8	7	15	22	25	8	15	22	20	12	15	22	25	9	15	22	23
P9	7	0	4	5	5	0	4	5	5	0	4	5	5	0	4	5
P10	8	3	16	10	5	3	16	10	5	3	16	10	38	3	16	40
P11	30	23	27	35	30	23	27	35	30	23	27	35	30	23	27	35
P13	57	0	7	60	57	0	7	60	57	0	7	53	63	0	7	60
P14	0	0	18	20	0	0	18	20	100	0	100	100	100	0	100	100
P15	41	0	5	43	48	0	10	48	48	0	10	48	82	0	10	75
P16	5	28	0	35	16	23	0	35	18	18	0	28	27	18	0	35
P17	67	33	10	60	67	33	10	60	67	33	10	60	67	33	10	60
P19	58	0	35	60	58	0	35	60	58	0	35	60	58	0	35	60
P20	39	0	7	38	39	0	7	38	39	0	7	38	39	0	7	38
P23	18	60	3	65	18	60	3	65	18	60	3	65	15	60	3	65
P24	33	0	0	38	33	0	0	38	38	0	0	43	35	0	0	38
P25	10	60	0	65	10	60	0	65	10	60	0	65	18	60	0	65
P26	26	0	23	38	26	0	23	38	26	0	23	38	35	0	26	53

Table 3 (*Continued*)

Pat.	Dose 1				Dose 2				Dose 3				Dose 4			
	GGO	HC	Ret	Total	GGO	HC	Ret	Total	GGO	HC	Ret	Total	GGO	HC	Ret	Total
P27	37	48	0	80	37	48	0	80	37	48	0	80	37	48	0	80
P28	16	0	13	10	16	0	13	10	16	0	13	10	16	0	13	10
P30	3	3	0	5	3	3	0	5	3	3	0	5	3	3	0	5
P31	65	0	53	75	72	0	53	78	72	0	53	78	72	0	53	78
P32	45	43	7	75	53	43	7	80	53	43	7	80	53	43	7	80
P33	40	0	37	65	52	0	37	73	52	0	37	73	52	0	37	73
P34	37	0	0	45	37	0	0	45	33	0	0	40	33	0	0	40

For 1 mm slice thickness (increment 1 mm).
For 2 mm slice thickness (increment 2 mm).
For 3 mm slice thickness (increment 2.4 mm).
For 5 mm slice thickness (increment 4 mm).

The overall analysis found no significant ($p < 0.36$ and $p = 1$, respectively) influence of dose on establishing the diagnosis. In detail, for reader 1 the second dose level was not significantly different ($p = 1$), dose level three and four showed p-values of =0.57 and $p = 0.12$, respectively.

The overall analysis found no significant ($p = 0.77$ and $p = 1$, respectively) influence of slice thickness on establishing the diagnosis. In detail, for reader 1 the 2 mm slice thickness resulted in a p-value of =0.6, 3 mm and 5 mm in $p = 0.6$ and $p = 0.29$, respectively.

Optimal LDCT series

The mixed model analysis allows for a combined analysis of dose and slice settings. The estimate of the linear model provides the offset compared to the optimal dataset; the closer this value is to zero, the better.

By using the aforementioned data, it was obvious that a dose level less than 2 leads to significant errors in rating of GGO and total disease extend. Therefore, this specific analysis was tailored to the slice thickness (Table 5). Using this approach, the least estimate (least difference from the original data set) was found for a combination of dose level 2 and slice thickness 5 mm for reader 1 and 3 mm for reader 2.

Discussion

In this study, we set out to establish an optimal LDCT protocol for the most common forms of chronic ILD, UIP and NSIP, by systematically evaluating LDCT imaging series with varying tube current and image slice thickness for differences in operating characteristics and imaging features. The evaluation was done with 2 readers, one experienced chest radiologist and one resident. A LDCT imaging series with 20 mA tube current (SD 30, respectively) and 3–5 mm slice thickness was most optimal, upholding diagnostic accuracy for pattern detection while delivering the lowest radiation dose. Further reductions in tube current to 10 mA resulted in significant reductions in image quality and increased estimation of disease extent, GGO and reticulation. These preliminary results provide support for applying a specific LDCT protocol in patients with common forms of ILD in larger, prospective studies.

Previous CT protocol studies comparing 150 mA versus 40 mA have found reduced sensitivity in detecting ILD imaging features, including interstitial opacities, reticulation, and GGO at lower tube currents.[14] We found estimated GGO, reticulation and disease extent to increase significantly with reductions in tube current to 10 mA. This is suspected to be as a consequence of reduced image quality with lower tube current, interpreted as an exaggerated burden of diseased lung. Image quality was also reduced in 1 mm slice series', compared with 3 mm and 5 mm, suggesting a higher number of images at low tube currents results in increased noise. Interestingly, we found little difference in disease extent and other imaging features between 50 mA and 20 mA series', suggesting a threshold exists, beyond which noise influences imaging feature interpretation. Accurately measuring disease extent on CT imaging is important, as it has been shown to predict functional decline and mortality in both CTD-ILD and IPF.[18,19]

The diagnostic accuracy of HRCT is quoted between 90 and 100% for UIP and 65 and 90% for NSIP, based on studies employing surgical-lung biopsy confirmation.[6,20,21] However, no studies have evaluated the diagnostic accuracy of LDCT imaging for distinguishing UIP and NSIP in comparison to HRCT. We found comparable agreement, sensitivity and specificity between all LDCT series for ILD pattern in comparison to HRCT. However, diagnostic accuracy was highest in 20 mA tube current series. This likely represents how challenging it can be to differentiate UIP and NSIP patterns, regardless of imaging protocol. A central feature in differentiating UIP and NSIP is the presence and extent of HC. We found no difference between LDCT series' in the reported extent of HC, which may explain why operating characteristics were preserved in the 20 mA series.

We compared LDCT series for diagnostic accuracy, image quality and estimated radiation dose to identify the optimal CT parameters. Diagnostic accuracy was felt to be the operating characteristic of principal importance, given it strongly influences the clinical diagnosis and decisions to initiate or withhold immunomodulating therapy. Image quality influences radiologist interpretation of imaging features. We found GGO, reticulation and disease extent to be highest in

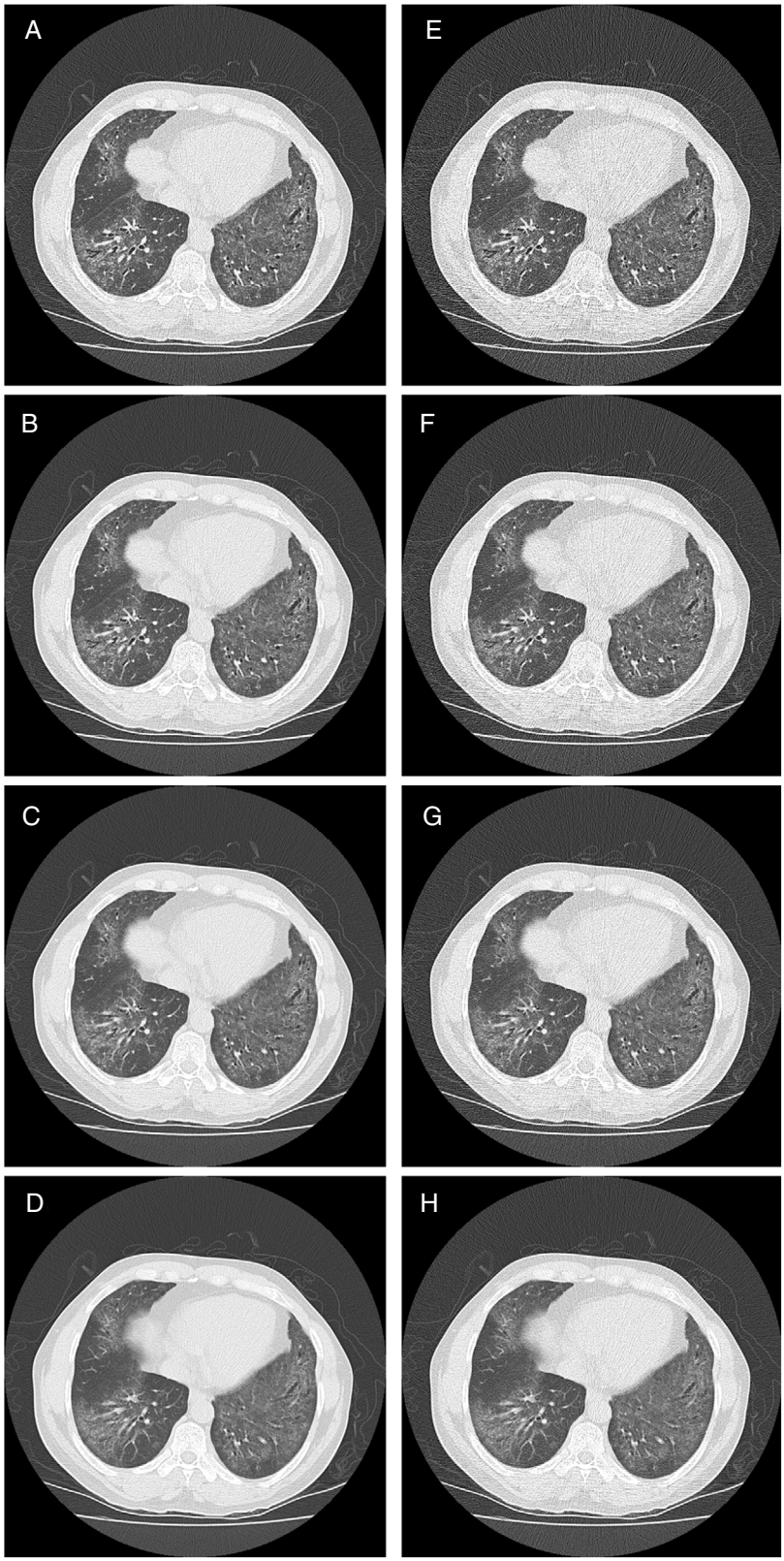

Figure 1 Presentation of ground appearance using 50 mA dose settings simulated 10 mA settings (E–H); images are displayed with W/L: 1600/−600 HU. 1 mm slice thickness (A and E), 2 mm slice thickness (B and F), 3 mm slice thickness (C and G) and 5 mm slice thickness (D and H).

Table 4 Statistical results for reader 1, reader 2, and combined of original and simulated CT datasets with respect to typical ILD features like ground glass opacities (GGO), honeycombing (HC), and reticulation (RET). Mean values were calculated using the SAS procedure ''GLIMMIX''. Also, total disease extend, image quality and diagnostic accuracy are shown.

	GGO	HC	RET	Tot disease	Image qual	Diagn
Reader 1						
Dose 1	–	–	–	–	–	–
Dose 2	=0.21	=0.29	=0.86	=0.61	<0.001	=1
Dose 3	=0.0003	=0.11	=0.85	<0.0001	<0.001	=0.57
Dose 4	<0.0005	=0.002	=0.14	<0.0001	<0.001	=0.12
Mean	<0.001	=0.002	=0.38	<0.001	<0.0001	=0.36
Slice 1 mm	–	–	–	–	–	–
Slice 2 mm	=1	=1	=1	=1	=0.08	=0.6
Slice 3 mm	=0.89	=1	=0.98	=0.98	<0.001	=0.56
Slice 5 mm	=0.19	=0.8591	=0.94	=0.17	=0.0002	=0.29
Mean	=0.248	=0.2966	=0.59	=0.024	<0.0001	=0.77
Dose*slice	=0.1	=0.93	0.48	=0.0078	=0.44	
Reader 2						
Dose 1	–	–	–	–	–	–
Dose 2	=0.01	=0.08	<0.0001	=0.0001	<0.0001	=1
Dose 3	<0.0001	0.0042	<0.0001	<0.0001	<0.0001	=1
Dose 4	<0.0001	<0.0001	<0.0001	<0.0001	<0.0001	=1
Mean	<0.0001	<0.0001	<0.0001	<0.0001	<0.0001	=1
Slice 1 mm	–	–	–	–	–	–
Slice 2 mm	=0.88	=0.82	=0.74	=0.86	=0.63	=1
Slice 3 mm	=0.46	=0.64	=0.7	=0.89	=0.59	=1
Slice 5 mm	=0.04	=0.02	=0.08	=0.07	=0.29	=1
Mean	<0.0001	=0.004	=0.006	=0.003	=0.08	=1
Dose*slice	=1	=0.97	=0.88	=0.97	=0.28	
Combined						
Dose 1	–	–	–	–	–	–
Dose 2	=0.01	=0.05	=0.003	=0.005	<0.0001	=1
Dose 3	<0.0001	=0.001	<0.0001	<0.0001	<0.0001	=0.67
Dose 4	<0.0001	<0.0001	<0.0001	<0.0001	<0.0001	=0.22
Mean	<0.0001	<0.0001	<0.0001	<0.0001	<0.0001	=0.56
Slice 1 mm	–	–	–	–	–	–
Slice 2 mm	=0.92	=0.84	=0.8	=0.9	=0.9	=0.68
Slice 3 mm	=0.55	=0.68	=0.77	=0.9	=0.03	=0.68
Slice 5 mm	=0.02	=0.03	=0.22	=0.8	=0.8	=0.4
Mean	=0.003	=0.01	=0.14	=0.002	<0.0001	=0.87
Dose*slice	=0.7	=0.85	=0.89	=0.1	=0.18	

the 10 mA series, which had the worst image quality. We suspect this is because increased noise leads to an exaggerated quantification of these imaging features. These preliminary results suggest protocols applying 10 mA tube current or less should be avoided, as this could lead to an overestimation of disease extent, and influence projected prognosis. We found the 20 mA/5 mm series to have the best balance of maintaining operating characteristics, while minimizing radiation exposure. However, given the detailed results for each parameter, it appears, that a slice thickness of 3 mm would show even less differences for the individual disease features.

Although there were only 28 subjects involved in this study, each CT performed was used to generate multiple data sets. Comparisons between LDCT series for the same patient removes individual inconsistencies (i.e. differences in breath holding) ensuring only protocol changes influenced CT interpretation. We limited our population to those with UIP and NSIP. This was done to create a homogeneous cohort, but limits the applicability of this protocol to ILD patients with other radiographic patterns. That said, IPF is the most common form of ILD and the approach to interpreting radiographic UIP outlined in ATS guidelines are often applied to those with undefined ILD [Raghu, 2011 #4452].[4]

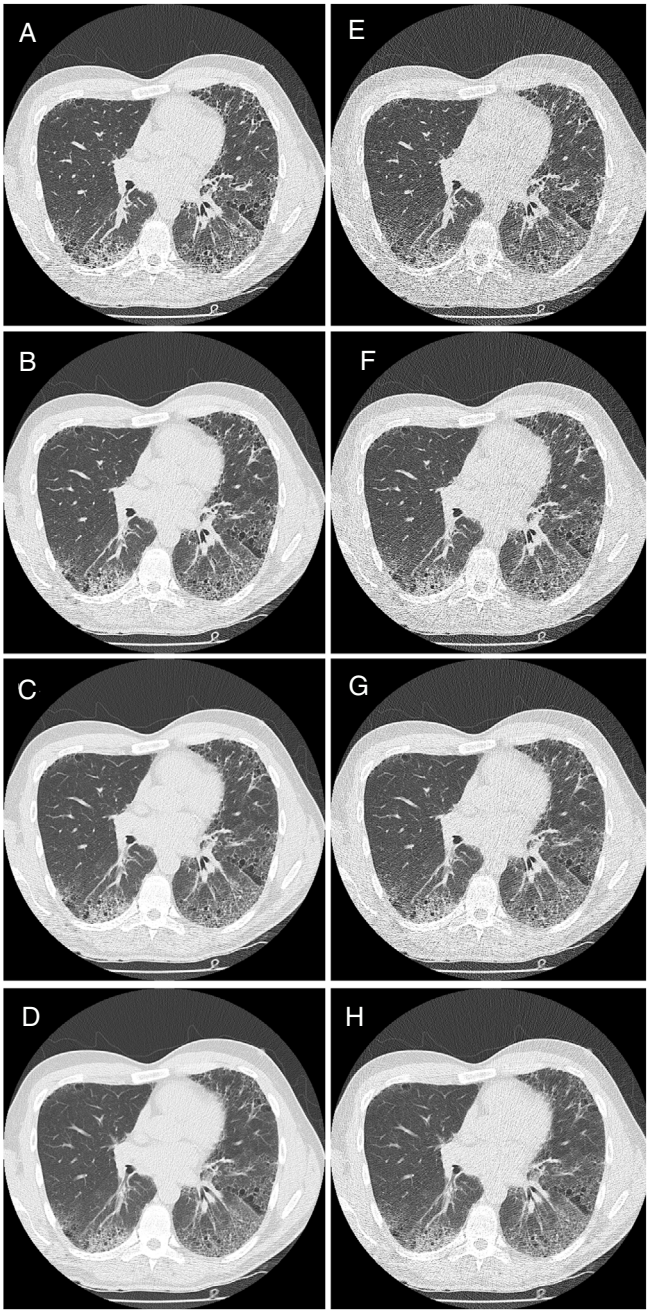

Figure 2 Presentation of reticulation using 50 mA dose settings (A–D) and simulated 10 mA settings (E–H); images are displayed with W/L: 1600/−600 HU. 1 mm slice thickness (A and E), 2 mm slice thickness (B and F), 3 mm slice thickness (C and G) and 5 mm slice thickness (D and H).

Our results suggest that LDCT imaging may accurately distinguish and characterize radiographic UIP and NSIP. A threshold appears to exist for LDCT parameters, below which operating characteristics are compromised. Most of the CT scanners use software-based dose modulation techniques for optimization of the image quality and radiation dose exposure. The dose limits can be adjusted be the user. In case an examination is too low dose due to a challenging body habitus, our results indicate, that it is possible to use even 3–5 mm slice thickness for compensation of the noise without losing the diagnostic capability of the examination (and to avoid re-scan). Additional studies investigating the diagnostic utility of various LDCT protocols in ILD are required.

Clinical relevance

- Low-dose CT imaging for diagnostic characterization of typical ILD changes with 20 mA possible.
- Slice thickness of 3 mm (increment 2.4 mm) and even 5 mm (increment 4 mm) does not impair evaluation of interstitial lung disease.

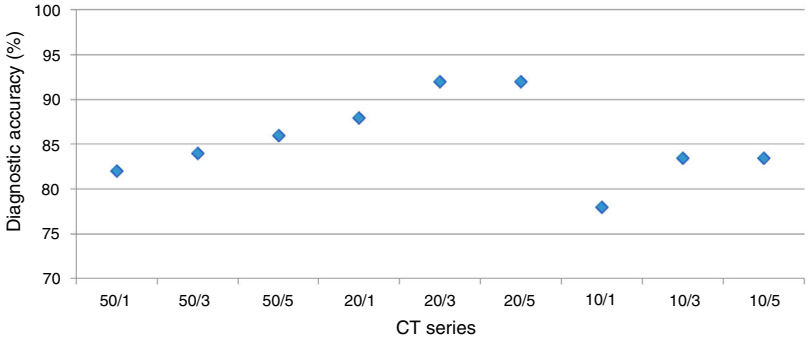

Figure 3 Diagnostic accuracy based on CT imaging parameters. CT series in milliamperes (mA)/millimetres (mm).

Table 5 Specific analysis of the influence of slice thickness on diagnostic accuracy. As ground glass opacities were the most susceptible parameter for the influence of reduced dose this parameter was chosen. For reader 1 and the combined analysis the estimate is closest to zero with the highest slice thickness of 5 mm, while 2 mm and 3 mm slice thickness were equal. For reader 2, a slice thickness of 3 mm showed the best sensitivity for detection of ground glass opacities in a reduced dose setting.

	Slice thickness	Estimate	*p*-Value
Reader 1			
Dose 2	2	−2.74	0.42
Dose 2	3	−2.93	0.38
Dose 2	5	−1.08	0.75
Reader 2			
Dose 2	2	−0.5	0.88
Dose 2	3	−0.0004	0.99
Dose 2	5	0.4	0.9
Combined			
Dose 2	2	−1.6	0.5
Dose 2	3	−1.5	0.6
Dose 2	5	−0.3	0.9

Funding

Own funding, no external funding.

Conflicts of interest

None declared.

Acknowledgements

We would like to thank Hatem Mehrez for data preparation, and Antonio Cassano for help with the manuscript revision and submission process.

Statistical analysis was performed by Dr. A. Crispin (The Institute for Medical Information Processing, Biometry, and Epidemiology; LMU Munich).

References

1. Solomon JJ, Ryu JH, Tazelaar HD, Myers JL, Tuder R, Cool CD, et al. Fibrosing interstitial pneumonia predicts survival in patients with rheumatoid arthritis-associated interstitial lung disease (RA-ILD). Respir. Med. 2013;107:1247–52, http://dx.doi.org/10.1016/j.rmed.2013.05.002. PubMed PMID: 23791462 [Epub 25.06.13].
2. Winstone TA, Assayag D, Wilcox PG, Dunne JV, Hague CJ, Leipsic J, et al. Predictors of mortality and progression in scleroderma-associated interstitial lung disease: a systematic review. Chest. 2014;146:422–36, http://dx.doi.org/10.1378/chest.13-2626. PubMed PMID: 24576924 [Epub 01.03.14].
3. Carrington CB, Gaensler EA, Coutu RE, FitzGerald MX, Gupta RG. Natural history and treated course of usual and desquamative interstitial pneumonia. N. Engl. J. Med. 1978;298:801–9, http://dx.doi.org/10.1056/NEJM197804132981501. PubMed PMID: 634315 [Epub 13.04.1978].
4. Raghu G, Remy-Jardin M, Myers JL, Richeldi L, Ryerson CJ, Lederer DJ, et al. Diagnosis of idiopathic pulmonary fibrosis. An official ATS/ERS/JRS/ALAT Clinical Practice Guideline. Am. J. Respir. Crit. Care Med. 2018;198:e44–68, http://dx.doi.org/10.1164/rccm.201807-1255ST. PubMed PMID: 30168753 [Epub 01.09.18].
5. Travis WD, Costabel U, Hansell DM, King TE Jr, Lynch DA, Nicholson AG, et al. An official American Thoracic Society/European Respiratory Society statement: update of the international multidisciplinary classification of the idiopathic interstitial pneumonias. Am. J. Respir. Crit. Care Med. 2013;188:733–48, http://dx.doi.org/10.1164/rccm.201308-1483ST. PubMed PMID: 24032382; PubMed Central PMCID: PMC5803655 [Epub 17.09.17].
6. Raghu G, Collard HR, Egan JJ, Martinez FJ, Behr J, Brown KK, et al. An official ATS/ERS/JRS/ALAT statement: idiopathic

pulmonary fibrosis: evidence-based guidelines for diagnosis and management. Am. J. Respir. Crit. Care Med. 2011;183:788–824, http://dx.doi.org/10.1164/rccm.2009-040GL. PubMed PMID: 21471066 [Epub 08.04.11].
7. Goh NS, Desai SR, Veeraraghavan S, Hansell DM, Copley SJ, Maher TM, et al. Interstitial lung disease in systemic sclerosis: a simple staging system. Am. J. Respir. Crit. Care Med. 2008;177:1248–54, http://dx.doi.org/10.1164/rccm.200706-877OC. PubMed PMID: 18369202 [Epub 29.03.08].
8. Assayag D, Elicker BM, Urbania TH, Colby TV, Kang BH, Ryu JH, et al. Rheumatoid arthritis-associated interstitial lung disease: radiologic identification of usual interstitial pneumonia pattern. Radiology. 2014;270:583–8, http://dx.doi.org/10.1148/radiol.13130187. PubMed PMID: 24126367; PubMed Central PMCID: PMC4228744 [Epub 16.10.13].
9. ACR-STR. ACR-STR practice parameter for the performance of high-resolution computed tomography (HRCT) of the lungs in adults; 2015. Available from: https://www.acr.org/-/media/ACR/Files/Practice-Parameters/HRCT-Lungs.pdf [cited 2018].
10. Brenner DJ, Hall EJ. Computed tomography – an increasing source of radiation exposure. N. Engl. J. Med. 2007;357:2277–84. PubMed PMID: 18046031.
11. Bouros D, Hatzakis K, Labrakis H, Zeibecoglou K. Association of malignancy with diseases causing interstitial pulmonary changes. Chest. 2002;121:1278–89. PubMed PMID: 11948064 [Epub 12.04.02].
12. McCunney RJ, Li J. Radiation risks in lung cancer screening programs: a comparison with nuclear industry workers and atomic bomb survivors. Chest. 2014;145:618–24, http://dx.doi.org/10.1378/chest.13-1420. PubMed PMID: 24590022 [Epub 05.03.14].
13. Winklehner A, Berger N, Maurer B, Distler O, Alkadhi H, Frauenfelder T. Screening for interstitial lung disease in systemic sclerosis: the diagnostic accuracy of HRCT image series with high increment and reduced number of slices. Ann. Rheum. Dis. 2012;71:549–52, http://dx.doi.org/10.1136/annrheumdis-2011-200564. PubMed PMID: 22121134 [Epub 29.11.11].
14. Christe A, Charimo-Torrente J, Roychoudhury K, Vock P, Roos JE. Accuracy of low-dose computed tomography (CT) for detecting and characterizing the most common CT-patterns of pulmonary disease. Eur. J. Radiol. 2013;82:e142–50, http://dx.doi.org/10.1016/j.ejrad.2012.09.025. PubMed PMID: 23122673 [Epub 06.11.12].
15. Zaporozhan J, Ley S, Weinheimer O, Eberhardt R, Tsakiris I, Noshi Y, et al. Multi-detector CT of the chest: influence of dose onto quantitative evaluation of severe emphysema: a simulation study. J. Comput. Assist. Tomogr. 2006;30:460–8. PubMed PMID: 16778622.
16. Gavrielides MA, Zeng R, Myers KJ, Sahiner B, Petrick N. Benefit of overlapping reconstruction for improving the quantitative assessment of CT lung nodule volume. Acad. Radiol. 2013;20:173–80, http://dx.doi.org/10.1016/j.acra.2012.08.014. PubMed PMID: 23085408 [Epub 23.10.12].
17. Hansell DM, Bankier AA, MacMahon H, McLoud TC, Muller NL, Remy J. Fleischner Society: glossary of terms for thoracic imaging. Radiology. 2008;246:697–722. PubMed PMID: 18195376.
18. Moore OA, Goh N, Corte T, Rouse H, Hennessy O, Thakkar V, et al. Extent of disease on high-resolution computed tomography lung is a predictor of decline and mortality in systemic sclerosis-related interstitial lung disease. Rheumatology (Oxford). 2013;52:155–60, http://dx.doi.org/10.1093/rheumatology/kes289. PubMed PMID: 23065360 [Epub 16.10.12].
19. Lee HY, Lee KS, Jeong YJ, Hwang JH, Kim HJ, Chung MP, et al. High-resolution CT findings in fibrotic idiopathic interstitial pneumonias with little honeycombing: serial changes and prognostic implications. Am. J. Roentgenol. 2012;199:982–9, http://dx.doi.org/10.2214/AJR.11.8192. PubMed PMID: 23096169 [Epub 26.10.12].
20. Johkoh T. Nonspecific interstitial pneumonia and usual interstitial pneumonia: is differentiation possible by high-resolution computed tomography? Semin. Ultrasound CT MR. 2014;35:24–8, http://dx.doi.org/10.1053/j.sult.2013.10.004. PubMed PMID: 24480140 [Epub 01.02.14].
21. Sumikawa H, Johkoh T, Fujimoto K, Arakawa H, Colby TV, Fukuoka J, et al. Pathologically proved nonspecific interstitial pneumonia: CT pattern analysis as compared with usual interstitial pneumonia CT pattern. Radiology. 2014;272:549–56, http://dx.doi.org/10.1148/radiol.14130853. PubMed PMID: 24661246 [Epub 26.03.14].